Accepted Manuscript

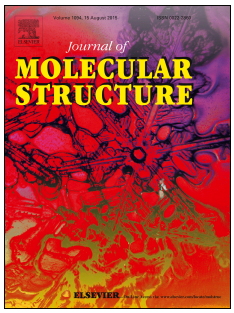

Crystal structure, Hirshfeld analysis and HSA interaction studies of *N*'-[(*E*)-(5-bromothiophen-2-yl)methylidene]-3-hydroxynaphthalene-2-carbohydrazide

Savithri K, BC Vasantha Kumar, Chandra, H.D. Revanasiddappa

PII: S0022-2860(19)30349-7

DOI: https://doi.org/10.1016/j.molstruc.2019.03.070

Reference: MOLSTR 26339

To appear in: *Journal of Molecular Structure*

Received Date: 8 November 2018

Revised Date: 16 March 2019

Accepted Date: 19 March 2019

Please cite this article as: S. K, B.V. Kumar, Chandra, H.D. Revanasiddappa, Crystal structure, Hirshfeld analysis and HSA interaction studies of *N*'-[(*E*)-(5-bromothiophen-2-yl)methylidene]-3-hydroxynaphthalene-2-carbohydrazide, *Journal of Molecular Structure* (2019), doi: https://doi.org/10.1016/j.molstruc.2019.03.070.

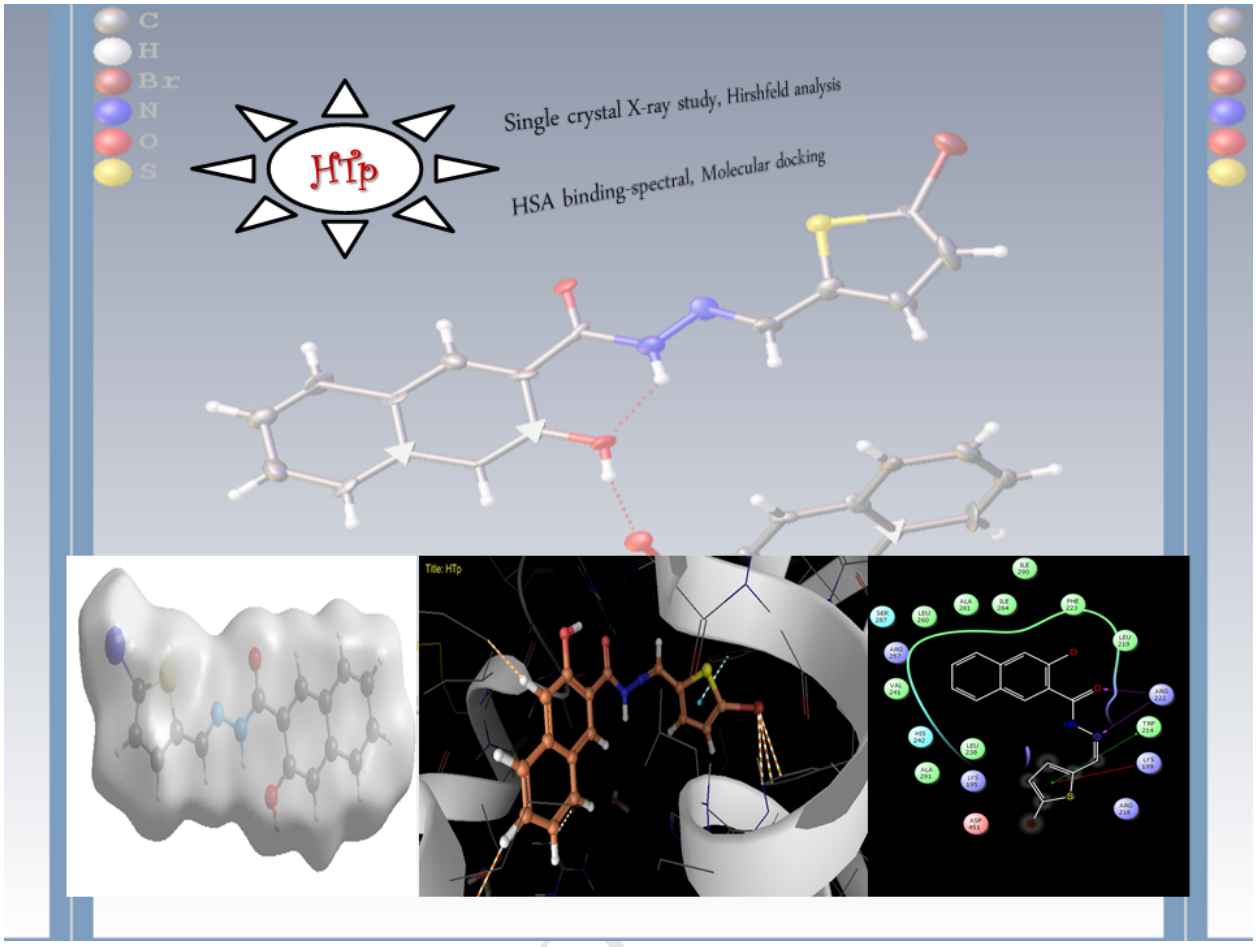
C
H
Br
N
O
S
HTp
Single crystal X-ray study, Hirshfeld analysis
HSA binding-spectral, Molecular docking
Title: HTp

Crystal structure, Hirshfeld analysis and HSA interaction studies of *N*'-[(*E*)-(5-bromothiophen-2-yl)methylidene]-3-hydroxynaphthalene-2-carbohydrazide

Savithri K[1], B C Vasantha Kumar[1], Chandra[2] and H D Revanasiddappa[1]*

[1]*Department of Studies in Chemistry, University of Mysore, Mysuru - 570 006, Karnataka, India*
[2]*Department of Physics, National Institute of Engineering (NIE), Mysuru- 570 008, India*
*Corresponding author. Tel.: +91 9449271137, *e*-mail: hdrevanasiddappa@yahoo.com

Abstract

Synthesis of ONO tridentate imine based molecule *N*'-[(*E*)-(5-bromothiophen-2-yl)methylidene]-3-hydroxynaphthalene-2-carbohydrazide (HTp) is gained quick attention because of its operational simplicity carried by both conventional and microwave methods and structurally it was elucidated by analytical, spectral, X-ray crystallography and Hirshfeld surface techniques. Analysis from the X-ray study provided the details of molecular structure, packing and hydrogen bonding properties in the solid state. The molecule is crystallized in monoclinic *P*21/*c* space group. The apparent binding affinity for the coupling of human serum albumin (HSA) with HTp drug molecule was examined through *in vitro* spectroscopic methods and molecular docking studies. HTp strongly quenched the intrinsic fluorescence intensity of HSA in terms of a static mode. The thermal based binding parameters were quantified from the fluorescence quenching experimental data. The energy transfer efficiency determined according to Förster's theory. Besides, the experimental results were in line with the molecular docking results.

Key points: Imine base; X-ray study; Hirshfeld analysis; Human serum albumin; Molecular docking;

1. INTRODUCTION

It is well known that the acid hydrazines R-CO-N=N-NH_2 and corresponding hydrazones R-CO-NH-N=CH-R' have interesting and remarkable biological activity among heterocyclic compounds due to their distinct physical, chemical and pharmaceutical properties. Nowadays, the N-N linkage is employed in various bioactive agents as a key structural motif [1]. It is well known that hydrazone compounds are a kind of distinct imine bases, which possess versatile chemical and pharmacological properties owing to their potential applications [2–8]**.** Aroyl hydrazones have stimulating ligation properties because of their facile keto-enol tautomerization and availability of several coordination sites [9–11]. The physiological effects of thiophene are similar to those of benzene (bioisostere), with habitually superior pharmacodynamics and pharmacological properties [12].

To accomplish the binding strategy of small molecules with the biomacromolecules have been received great importance. Human serum albumin, the principal extracellular ubiquitous blood serum constituent (~60 % of total plasma protein) serves as the major transporter, play physiological role in bringing solutes into the bloodstream, deliver them to the target site and maintain the optimal pH range 4-9 as long as 10 h at 60 $^{\circ}$C [13-15]. A multi-domain structure (Sudlow's sites) of HSA accounts for high binding affinity to the various chemical entities which is also a prerequisite factor for the application with the biological drug molecules and make the protein a chief regulator of intercellular metabolic and the pharmacokinetic behavior of many drugs in the body as well [16]. Hence, the molecular structural features of HSA based drug delivery systems invariably provides information on the therapeutic effect of a compound and have an immense interest in the development of biologically active new compounds. Drug-protein interaction effects on the drug absorption, circulation and abolition in the circulatory system. The binding efficiency of the ligands to serum albumin is believed to affect their half-life [17]. Moreover, such binding helps to increase drug solubility in plasma by preventing rapid exclusion of drugs from the bloodstream, decreases its toxicity and prolong it's *in vivo* half-time with the protection from the oxidation [18].

The exigency of the binding process of the imine based ligand (HTp) with HSA in providing potential drugs is the target that the author had. This was achieved using absorption, emission spectroscopy and molecular modeling under simulated physiological conditions. The employed UV-Vis and fluorescence spectroscopic techniques were

adequate to study the binding behavior of ligands with proteins due to its sensitivity, reproducibility and convenience. The binding parameters, thermodynamic functions and fluorescence resonance or Forster's non-radiative energy transfer (FRET) on the protein microenvironment were interpreted. Furthermore, it was curious to locate the binding sites of ligands on HSA, and this was able to identify the pose of the molecules in the binding sites by using docking tools and the binding score represents the strength of binding affinity.

2. EXPERIMENTAL

2.1. Instruments and operations

All the used chemicals throughout the experiments were of reagent grade. A precision digi melting point apparatus was used to determine the melting point of HTp in an open capillary tube. For the structural identification, an Agilent NMR spectrometer was used to record ^{1}H and ^{13}C NMR spectra with TMS as a reference in DMSO-d_6 solvent at ambient temperature. LCMS (2010EV) Shimadzu spectrometer was employed to record the mass spectrum. CHN microanalysis was performed with a Perkin-Elmer elemental analyzer. UV measurements (200-800 nm) were performed with UV-Vis spectrophotometer (DU 730 M/S Beckman coulter, 'Life Science' USA) using DMSO solvent. Vibrational spectra were recorded *via* attenuated total reflection (ATR) on a Perkin-Elmer 783 spectrophotometer in the range of 4000-400 cm^{-1}.

2.2.Synthetic procedure of compound (HTp):

N'-[(E)-(5-bromothiophen-2-yl)methylidene]-3-hydroxynaphthalene-2-carbohydrazide

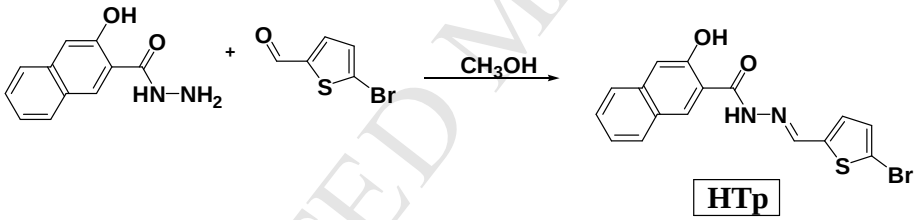

Scheme 1

Classical method

A methanolic solution of 5-Bromo-2-thiophenecarboxaldehyde was added to a well-stirred methanolic solution of 2-amino-3-hydroxy-2-naphthoic acid hydrazide in an equivalent ratio. The reactant mixture was continued to stir for an hour at room temperature (26 $^{\circ}$C), during which a creamy white precipitate was formed and TLC was utilized to monitor the reaction. The solid product was recrystallized with the solvent system of methanol and chloroform (3:7) by a slow evaporation method. **Yield**=83 %.

Microwave irradiation method

An equivalent reaction mixture of the 2-amino-3-hydroxy-2-naphthoic acid hydrazide and 5-bromo-2-thiophenecarboxaldehyde was placed in a flask and subjected to microwave power at 300 W with the temperature of 80 °C for ~6 minutes. TLC monitored the completion of the reaction and the content was left for evaporation at ambient temperature (26 °C). The colorless crystalline product was formed from the recrystallization of methanol/chloroform (3/7) system. **Yield**=89 %.

Mp= 224-226 °C; **R_f** 0.55, **Anal. (%)** for $C_{16}H_{11}BrN_2O_2S$: **Found (calc.):** C 51.20 (51.21), H 2.92 (2.95), N 7.43(7.47); **LCMS m/z** 375.23; FT IR ($\upsilon_{max.}$/cm^{-1}); (HC=N) 1663, (υOH) 3253; **^{1}H NMR (**DMSO-d_6 400 MHz/295 K/δ in ppm) 9.776 (s, 1H, HC=N); 10.04 (s, 1H, OH), 11.16 (s, 1H, NH), ppm 7.21-7.26 (m, 2H, Ar); **^{13}C NMR** (DMSO-d_6 100 MHz) 154.333, 164.039, 143.132, 141.273, 136.257, 132.220, 131.810, 130.664, 129.070, 128.645, 127.219, 126.278, 124.236, 120.981, 115.509, 110.994.

2.3. X-ray structure determination protocol

The titled imine based molecule $C_{16}H_{11}BrN_2O_2S$ has been synthesized; high-resolution X-ray diffraction determines its crystal structure. The analysis provided the details of the molecular packing and hydrogen bonding of HTp.

A single crystal of *N*'-[(*E*)-(5-bromothiophen-2-yl)methylidene]-3-hydroxynaphthalene-2-carbohydrazide (HTp) with dimension 0.30× 0.25 ×0.20 mm was chosen for diffraction studies. The crystallographic X-ray diffraction data were collected at 296 K on a Bruker APEXII CCD detector with CuKα radiation (1.54178 Å). Processing and reduction of crystal structure raw data were carried out using APEX2 and SAINT [19]. A crystal structure of HTp was solved by direct methods; full-matrix least-squares refinement was performed using SHELXS-97 and SHELXL-97 [20, 21] with a final residual value of R_1=0.045. The thermal ellipsoid plot [22] at 50% probability of the compound is publicized in crystallographic figures.

2.3. Hirshfeld surface analysis

Analysis of molecular crystal structure by Hirshfeld method to venture crystal packing diagrams of various models, internuclear distances and angles, hydrogen bond interactions and credentials of close contacts deemed to be significant given molecule as

organic wholes; thereby the crystal lattice can be stabilized. *Crystal Explorer 3.0* [23] computational software was employed to perform Hirsh surface analysis.

2.4. Preparation of HSA stock solution

Human serum albumin (HSA, >99% purity, essentially globulin free) was procured from Sigma Aldrich Inc. An initial solution of HSA was prepared by dissolving and dialyzed it in a buffer (Tris-HCl/NaCl at pH 7.4) prior to use, and it was kept at 4 °C for no longer than two days. The standard working solutions of 0-25 µM were made the stock.

HSA concentration in buffer was determined by UV absorbance with $\sum_{280nm}^{1\%}$ is 35700 $M^{-1}cm^{-1}$ [24].

2.4.1. Electronic absorption and Fluorescence spectral measurements

The UV-Visible spectra were recorded with a quartz cell of 1 cm path length. Absorption spectra of HSA-HTp were scanned from 200 to 800 nm with concentration ranges from 0-25 µM at ambient temperature.

Steady-state fluorescence spectral measurements were recorded on F-2000 spectrofluorometer, Hitachi equipped with a 150 W Xenon lamp at 298, 303 and 310 K. Very dilute solutions of HSA (2×10^{-6} mol/L) and HTp ($0\text{-}6\times10^{-6}$ mol/L) were taken. The excitation wavelength was made to fix at 295 nm, while the emission wavelength measured from 300 to 500 nm with a slit width of 5 nm. The Origin 7.0 software provided with Microcal was employed to analyze the titration heat profiles to find binding parameters. Data well fitted to a single set of identical binding parameter [25].

The inner filter effect could stand as an error for any fluorescence measurement particularly where an absorbing component is being titrated into the cuvette [26]. An absorption spectrum of the ligand overlaps with the excitation and emission of HSA. Hence, Inner filter effect and dilution effects were corrected for fluorescence intensities before binding and quenching data analysis. Fluorescence intensity was corrected based on the Eq. (1)

$$\mathbf{F_{corr}} = \mathbf{F_{obs}}\, e^{(\lambda_{ex}+\lambda_{em})/2} \qquad \ldots\textbf{(1)}$$

The corrected and observed fluorescence intensities are referred to as F_{corr} and F_{obs}, respectively and $\boldsymbol{\lambda}_{em}$ and $\boldsymbol{\lambda}_{ex}$ are the absorption of HTp at the emission and excitation wavelength of HSA. All the HTp solutions were prepared by weight/volume (w/v) basis.

The fluorescence quenching phenomena are conventionally described in terms of Eq. (2) given by Stern-Volmer [27].

$$\frac{F_0}{F} = 1 + K_{sv}[Q] = 1 + K_q \tau_o [Q] \qquad \ldots (2)$$

where, the quenched fluorophore intensity and the steady-state fluorescence intensity are represented by F and F_o, respectively. [Q] is the molar concentration of HTp, Stern-Volmer quenching constant is given by K_{sv} and k_q is the apparent biomolecular quenching rate constant. τ_o stands for the integral/average lifetime of protein fluorophore without quencher and the fluorescence lifetime of the biomolecule is 10^{-8} s [28, 29].

Energy transfer between HTp and HSA

Energy transfer between HTp and HSA gives valuable information about their binding. Equimolar concentration (10^{-6} mol L^{-1}) of the absorption spectra of ligands and the fluorescence spectrum of HSA were recorded at 298 K with the range from 200 to 500 nm (n=3 replicates). Then, the overlap of the UV absorption spectrum of HTp with the emission spectrum of HSA was used to calculate the energy transfer and subtracted the buffer background readings.

2.5. Molecular docking studies

AutoDock was employed for docking simulation. The crystal structure of the *N*'-[(*E*)-(5-bromothiophen-2-yl)methylidene]-3-hydroxynaphthalene-2-carbohydrazide (HTp) was selected for docking study with receptor Human Serum Albumin target, obtained from the protein data bank (PDB Code: 1H9Z). The AutoDock has to contain core technology, which is used for simulations of bio-organics and macromolecules. Simulations are an essential tool to validate HTp pose geometries, stability and the generation of macromolecule conformations. For the docking methodology, Lamarckian genetic algorithm was used to figure out the optimal docking position between small molecules and macromolecules. Also, partial atomic charges were calculated using Gasteiger method. AutoDock tools (ADT) was used to define the rotatable bonds in the ligand. In addition to that, both Kollman charges and polar hydrogen bonds were assigned using ADT.

3. Results and Discussion

3.3. Chemistry

A potential imine-based molecule (HTp) was synthesized (Scheme 1) by two ways where microwave assisted synthesis is more accessible, convenient and have short reaction period. The obtained yield (89%) from this was found to be much more than the conventional method (83%). The product HTp is stable at atmospheric conditions, non-hygroscopic and moderate solubility in alcohol but highly soluble in hot alcohol and all common organic solvents. Analytical data of the compound are reliable with the proposed formula and are summarized in the above synthetic section.

The ^{13}C NMR spectrum of HTp is displayed in **Fig. S1**† shows a characteristic signal at 143.132 ppm for the azomethine (HC=N) carbon. The chemical shift positions of other carbons have appeared at 159.638, 158.848, 135.710, 124.494, 121.596, 115.471 and 109.150 ppm. A singlet signal peaked at 9.77 ppm in ^{1}H NMR spectrum of HTp is attributed to the azomethine proton. The OH proton resonates as a singlet equivalent to single hydrogen at 10.04 ppm indicates that the OH proton is probably involved in the formation of intramolecular hydrogen bonding. NH proton appears at11.16 ppm and aromatic protons are resonated as multiplet in the range of 7.0-7.92 ppm. The molecular ion peak at m/z 375 [M] and 376 [M+1] in the mass spectrum of HTp corresponding to its formulation and confirms the presence of bromine in the molecule. The IR spectrum of the molecule exhibits a sharp band at 1662 cm^{-1} due to the azomethine group (HC=N) vibration. Some significant stretching bands associated with N-H, C=O, C=N and O-H were observed in the range 3339-3175, 1630–1660, 1610-1635 and 3490-3515 cm^{-1}, respectively [9,30]. Also, a new C–O stretch has appeared in the range 1260–1285 cm^{-1}. It suggests the occurrence of keto-imine tautomerization of hydrazone groups. The electronic spectrum **(Fig. S2†)** of HTp show intense bands in the range 320-385 nm attributed $\pi \rightarrow \pi^*$/n $\rightarrow \pi^*$ transitions.

3.3.1. Crystal features of HTp

The X-ray crystal and molecular structure analysis of the compound (HTp) suggested that the compound crystallizes in monoclinic system under the space group *P*21/c, with cell parameters a = 16.5155(19)Å, b = 11.4248(14)Å, c = 7.9982(10)Å, β = 92.993(4)Å and Z=4. **Table S1**† detailed the crystal data and structure refinement for HTp. In the Oak Ridge thermal ellipsoid plot (ORTEP) drawn for the HTp molecule (**Fig. 1**), the thermal ellipsoids for naphthalene (C1—C10) and thiophene groups (S1—C13—C14—C15—C17) are almost

collinear as appears from the relative dihedral angle of 1.70(12)° between the two groupings. The hydroxyl group and bromine moiety are approximately coplanar with the naphthalene and with atom O1 and Br1 deviating from the mean plane by -0.047 (2) Å and -0.019 (1) Å, respectively. Also, carbohydrazide group is present in anti-periplanar conformation relating to the naphthalene moiety, as indicated by the torsion angle value of -179.9 (2)° (N2—N1—C11—C10). The crystal structure is stabilized by N(1)—H(1A)...O(1) intramolecular H-bonds. The packing of the molecules is as shown in **Fig.S3†.**

3.3.2. Hirshfeld surface analysis

The molecular Hirshfeld surface (3D d_{norm} surface, shape index and curvedness) is displayed in **Fig.2.** The deep red spot with large circular depressions visible on the normalized contact distance (d_{norm}) surfaces with d_i and d_e indicates hydrogen bonding and other weak contacts. The shape index displays red areas parallel to C-H-C (or C-H--π) interactions, which coincide with similar regions in the d_{norm} surface. The van der Waals (vd_W) radii encodes particularly for intermolecular interactions [31]. The shape index is extremely sensitive to subtle variations in the surface shape and is consistent with 2D fingerprint plots. The curvedness is usually tending to divide the surface into patches, indicates neighboring molecular interactions [32]. The two-dimensional fingerprint plots further emphasized the significance of the H--H, C--H, O--H, S--H and H--Br interactions in determining its arrangement in the solid state. The significant contribution obtained from the interactions which make up C—H (15 %) and H—H (22.8 %) of the surface. Quantification of different interactions and their relative contributions are displayed in **Fig. 3.**

3.4. HSA Binding studies

UV–Vis spectral features

The simple but effective method to study the HTp-HSA binding and to investigate the structural modification of the aromatic protein residues upon drug accumulation is UV-Vis/electronic absorption spectroscopy. As can be seen in **Fig. 4,** a sharp absorption peak at ~206 nm resulted by n to π^* transition for the peptide bond of protein helix and a weak peak at 278 nm is assigned to π to π^* spin forbidden transition of the phenyl rings in aromatic amino acids Trp, Tyr and Phe residues [33]. A hypochromic effect is observed **(Fig. 4**) in the

absorption spectrum of HSA on gradual incremental addition of compound HTp (10 µM), the reduced absorption intensity of HSA after the enhancement of HTp implied that the aromatic amino acid residues of the protein in a hydrophobic cavity were exposed to an aqueous environment upon complexation of HTp with HSA and could cause structural changes in the protein.

Fluorescence spectral analysis

Fluorescence titration is a qualitative spectroscopic technique of the binding of the drug to the proteins. Fluorescence titration is a qualitative spectroscopic technique to obtain the details on the binding of the drug to the proteins, binding sites and intermolecular distances exists between them. The fluorescence quenching is any process which diminishes the fluorescence intensity of a compound. The quenching can be the consequence of a variety of molecular interactions may include excited-state/ground state complex reactions, energy transfer or collisional quenching. The fluorescence quenching of ligands and HSA is due to the intrinsic tryptophan residue, which is used as an inherent probe to comprehend the interaction of ligands with the protein as the other two aromatic fluors *viz.* tyrosine and phenylalanine have meager quantum yield which undergoes ionization when they locates close to carboxyl groups, so they get quenched completely [15].

The fluorescence quenching of HTp and HSA is due to the intrinsic tryptophan residue, which is used as a prime tool to understand the interaction of HTp with the protein **(Fig. 5).** While titrating HTp with HSA, the maximum fluorescence intensity at 342 nm was decreased with the addition of the compound continues, which leads to changes in the microenvironment around tryptophan-214 when excited at 295 nm. The above data specifies that the HTp binding site exists near to the tryptophan residue, which is located at the IIA subdomain of HSA.

Diverse molecular interactions may results in fluorescence quenching of intrinsic fluorophore due to energy transfer, molecular rearrangement and collision quenching. The observed fluorescence quenching is likely related to collisional quenching by the ground state complex formation when the inner filter effect is removed [34]. Fluorescence quenching can be static or dynamic type according to their different temperature dependence. Hence, fluorescence tests were performed at temperatures (298, 303 and 310 K) and the quenching

data were analyzed using Stern-Volmer (SV) plot expressed in equation **(2).** SV quenching plot of F_o/F *v/s* [Q] shown in **Fig.5** helps to get the values for K_q and K_{sv}. The binding parameters with a correlation coefficient (R^2) at chosen temperatures are tabulated in **Table 1.** K_{sv} reflects the efficiency of fluorescence quenching which is given by the slope. The linear regression of the SV plot proposes the binding process of HTp to HSA is indicative of homogeneity of quenching and the phenomena found to be 'static' since the observed K_{sv} values drastically decreased on raising the temperature with high magnitude of k_q (10^{12} $M^{-1}S^{-1}$) is found. The dynamic quenching occurs when the quencher and fluorophore approach each other at excited state, while static quenching occurs when non-fluorescent complex formed in the ground state.

3.4.1. Analysis of binding equilibria

Fluorescence quenching data analysis afforded quantitative evaluation of the binding constant (K_b) and binding stoichiometry (n) for the HSA-HTp interaction process and analyzed according to modified Stern-Volmer Eq. (3)

$$\log\left[\frac{F_0-F}{F}\right] = \log K_b + n\log[Q] \ldots \textbf{(3)}$$

where, the quenched fluorophore intensity and the steady-state fluorescence intensity are represented by F and F_o, respectively. The double logarithm regression plot of $\log(F_o\text{-}F)/F)$ *v/s* log[Q] is shown in **Fig. S4†,** where slope and intercept gives K_b and n, the values of the same at performed temperatures are reported in **Table 1.** It was observed that the binding constant (K_b) decreases as temperature rises which indicates the formation of unstable HSA-HTp complex.

The values of n are observed to be close to unity indicating that there is one independent class of binding site on HSA available for HTp. The thermodynamic parameters for the HSA-HTp interaction process have also been estimated from the binding constant. The analysis of binding isotherms gives the major binding parameters that fit as a function of the binding constant K, ΔS^o (entropy of association) and ΔH^o (enthalpy of association) of the protein.

In general, the non-covalent nature of binding forces exists between quencher and macromolecules. Hydrogen bonds, van der Waals force, hydrophobic force and electrostatic forces are the four major molecular acting forces of interaction exists between HSA and HTp. Thermodynamic analysis of protein-HTp binding shows the importance of the binding

constant (K), entropy change (ΔS), enthalpy change (ΔH) and free energy change (ΔG) in determining the predominant type of interactions in HTp–protein complex system [35] and were used to elucidate probable binding forces of drug-protein interactions and these can be intended by Van't Hoff and thermodynamic eq. (4) and (5) [36].

$$\ln K_{bin} = -\frac{\Delta H^\circ}{RT} + \frac{\Delta S^\circ}{R} \quad \ldots\textbf{(4)}$$

$$\Delta G^\circ = \Delta H^\circ - T\Delta S^\circ = -RT\ln K_{bin} \quad \ldots\textbf{(5)}$$

in which, K_{bin} is apparent binding constant, T is the absolute temperature and R is gas constant (1.987 cal/mol·K). Slope and intercept of the plot of logK *v/s* 1/T (**Fig. S5†)** gives ΔH° and ΔS°, respectively. Gibbs-Helmholtz equation 5 helps to calculate ΔG° and the results are summarized in **Table 2.** A spontaneous and exergonic binding process observed through the negative free energy change.

The obtained negative ΔH° (-78.314 $KJmol^{-1}$) and ΔS° (-361.304 $KJmol^{-1}$) indicate predominant interactions in the binding process [37]. The compound HTp could actively quench the intrinsic fluorescence of protein as the decreasing values of the binding constant with an increase in temperature leads to the decrease in the stability of the HSA-HTp complex which in turn suggests static quenching mechanism. Indeed, the unfavorable enthalpy loss is canceled by the much larger entropic gain reveals hydrogen bonding and weak van der Waals forces played a significant role in the interaction.

3.4.2. Resonance energy transmission between HSA and HTp

The significance of the energy transfer in biochemistry is that the efficacy of transmission can be used to measure the distance between the ligand and the tryptophan residues in the HSA. To find out a distance between HTp-Trp protein, it is possible to study Forster's non-radiative process or fluorescence energy transfer (FRET) from donor (HSA) to acceptor (HTp). FRET occurs when the fluorescence spectrum of HSA (fluorophore) overlays on the UV absorption spectrum of HTp (acceptor) and is displayed in the **Fig.S6†**. HSA has a solitary tryptophan residue (Trp 214) which gives a fluorescence emission at 300-400 nm.

As per the FRET theory [38], the energy transfer efficiency (E) is given by Eq. (6) and (7) which is interrelated to the distance (r) from donor to acceptor and the critical energy transfer distance when *E* is 50 % is known as Forster's radius (R_o).

$$E = 1 - \frac{F}{F_0} = \frac{{R_0}^6}{{R_0}^6 + r^2} \ldots \textbf{(6)}$$

$${R_0}^6 = 8.79 k^2 N^{-4} J \varphi N^{-4} \quad \ldots \textbf{(7)}$$

where, the donor's fluorescence quantum yield Φ_D is 0.15, the orientation factor k^2 =2/3, and the refractive index (n=1.336) were obtained. The overlap integral of the absorption spectrum of the HTp and the fluorescence emission spectrum of the HSA termed as J, and is given by the Eq. (8)

$$J = \frac{\Sigma F_D(\lambda)\varepsilon_A(\lambda)\lambda^4 d\lambda}{\Sigma F_D(\lambda) d\lambda} \ldots \textbf{(8)}$$

where, the fluorescence intensity of the donor at wavelength λ is termed as $F_D(\lambda)$ and the acceptor's molar absorption coefficient at λ wavelength is $\varepsilon_A(\lambda)$

We observed a functional overlap between the emission spectrum of tryptophan and the absorption spectrum of HTp **(Fig. S5†).** The values for J=4.67×10^{-14} cm^3 $Lmol^{-1}$, E=0.17, R_o=2.49 nm and r=4.26 nm which were easy to obtain by using the equation 8.

These obtained data are consistent with a FRET mechanism being operative. *i.e.* The r value is actually the average value between the bound drug and Trp214 (since HSA possess only one tryptophan residue) and is found to be less than the standard value of 8 nm or on 2-8 nm scale and 0.5 R_o < r < 1.5 R_o indicates a significant spectral overlap occurs between HSA-ligands with high probability. Further, as per the prediction by Forster's non-radiative energy transfer theory, the more substantial value of r compared to that of R_o proves the static quenching process [39, 40].

2.3.1. Molecular modeling study

The analysis was performed to decode the binding site of HTp against HSA. Crystal structure of monomeric albumin revealed that the single polypeptide chain of heart-shaped HSA consists three structurally homologous α-helical domains I(residues 1-195), II (196-33) and III (34-585 amino acid residues) and each of the domain contains two subdomains A and B, stabilized by 17 S-S bridges [41].

Using molecular docking simulations, the imine based ligand HTp was docked to the best conformer of HSA and they generally found to bind within their hydrophobic pockets in subdomains IIa and IIIA, such as site I and site II. The molecular docking analysis signified the most critical regions of compound binding sites in the HSA. The ligand molecule (HTp)

showed minimum binding energy of -7.5 kJ/mol with ligand efficiency -0.34. HTp molecule shows hydrogen bond interaction with active site amino acid residues Arg257 and His288 at a distance of 1.904 Å, 2.174 Å & 1.882 Å respectively. The molecular modeling results revealed that the compound (HTp) have a good inhibition constant, vdW+H_{bond}+desol energy with the best root mean square deviations. The best energy ranked details of the interaction between the HTp and the receptor human serum albumin target (PDB Code: 1H9Z) in all the runs of docking protocol have listed in **Table S2†.** Enfolding and H-bond interaction of molecule (HTp) are in the active site pocket of serum albumin target (PDB Code: 1H9Z) as shown in **Fig. 6A** and **Fig. 6B.**

4. CONCLUSION

We report the convenient synthesis of a tri-dentate imine based molecule (HTp) in good yield. The molecular structure was well explored through crystallography, Hirshfeld surface analysis and several spectroscopic techniques. As the key circulating protein in the blood, albumin serves the excellent delivery platform for many exogenous and endogenous compounds. The nature of the binding of synthesized HTp with HSA was studied using fluorescence and UV-Vis absorption method under physiological conditions. The interactions were confirmed through variations in the absorption spectra and intrinsic fluorescence quenching of the HSA. Further study of the quenching process uses k_q, k_{sv} and k_b parameters and the higher values of K_b demonstrated strong interaction with HSA. The probable mode of interaction strategy is found to be a static quenching process.

FRET and fluorescence quenching model afforded the distance between the HSA and HTp being the ratio 1:1 suggests that the high possibility of energy transfer has occurred. HSA had a crucial effect on drug distribution and pharmacokinetics as the compound could quench the protein fluorescence through static quenching phenomena. Quantitative assay for the binding of HTp with HSA was proposed from multi-spectroscopic methods at different temperature conditions and correlated by molecular docking technique. With the above data provided, this will be the benchmark for the molecule HTp to get used for further clinical applications in protein conjugation pharmacology.

APPENDIX

CCDC 1548542 contains a supplement of crystallographic data for HTp.

ACKNOWLEDGMENTS

One of the authors, Savithri K gratefully acknowledges the University Grants Commission, New Delhi for the award of Senior Research Fellowship under RGNF Scheme.

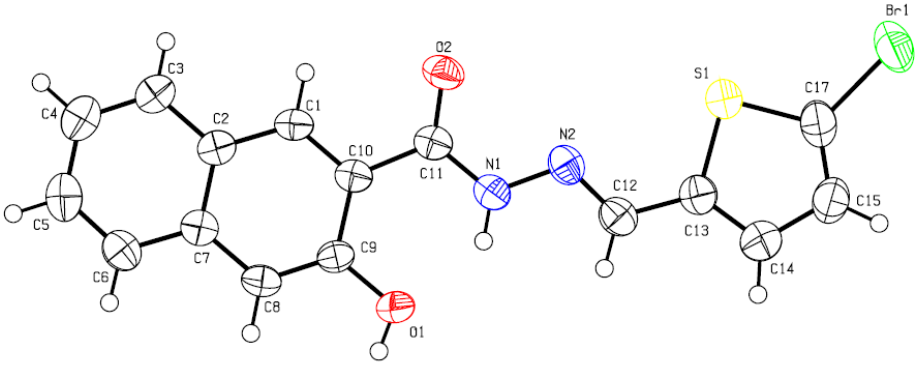

Fig.1. Ortep representation of HTp

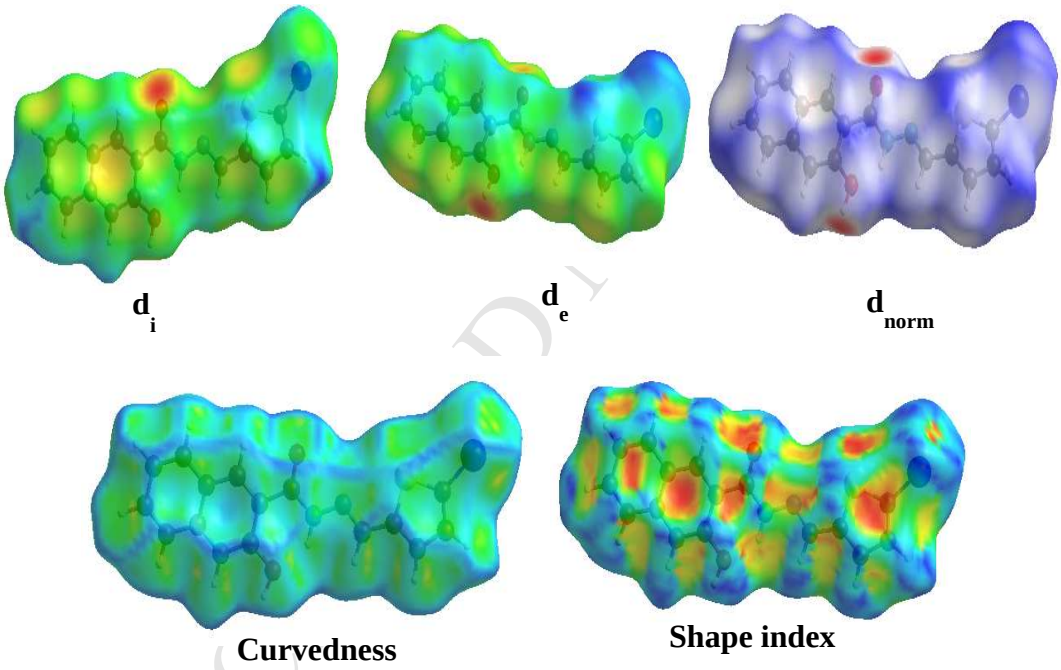

Fig.2. $3d_{norm}$ surface, shape index and curvature mapped on Hirshfeld surface of HTp

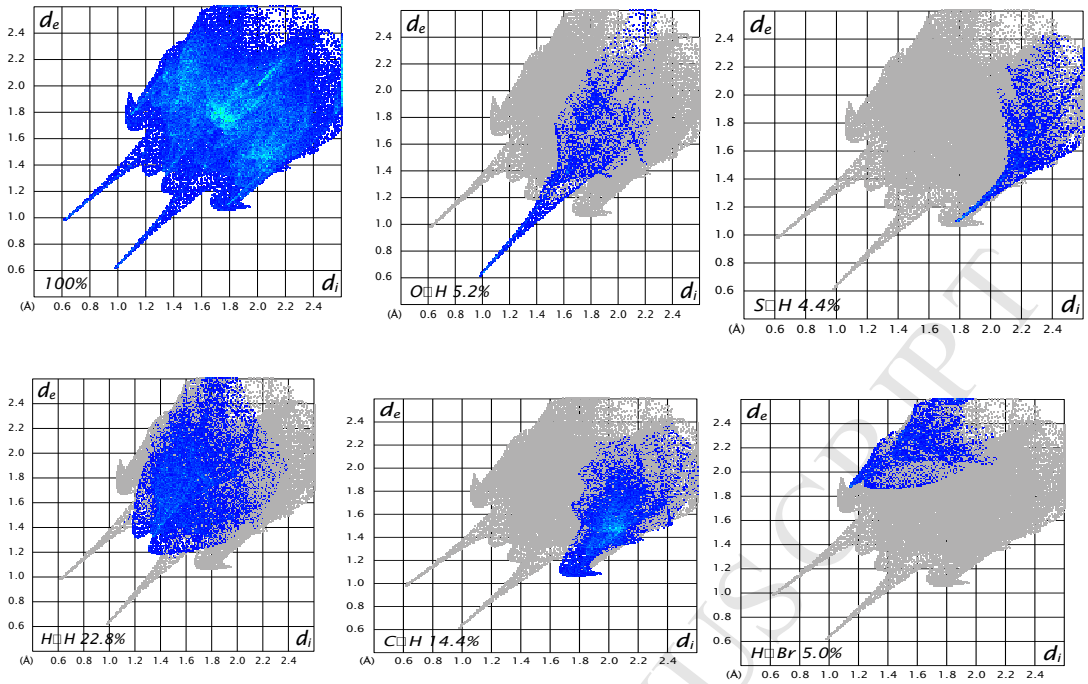

Fig.3. Fingerprint plot of the HTp.
Various contacts contributing to the total Hirshfeld surface of HTp molecule.

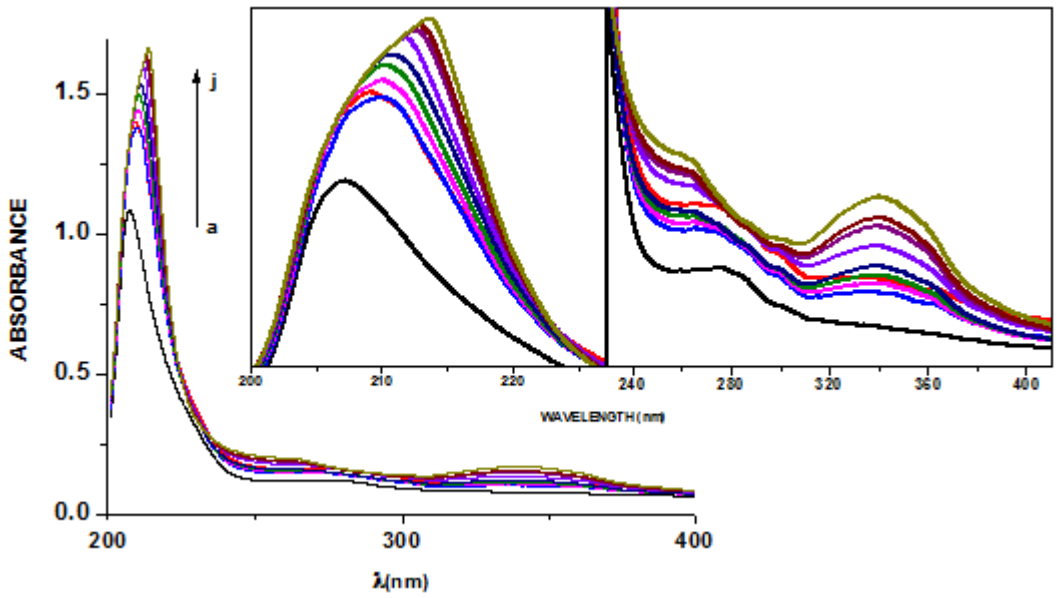

Fig.4. UV absorption spectra of HSA in the absence and presence of varied concentrations of HTp

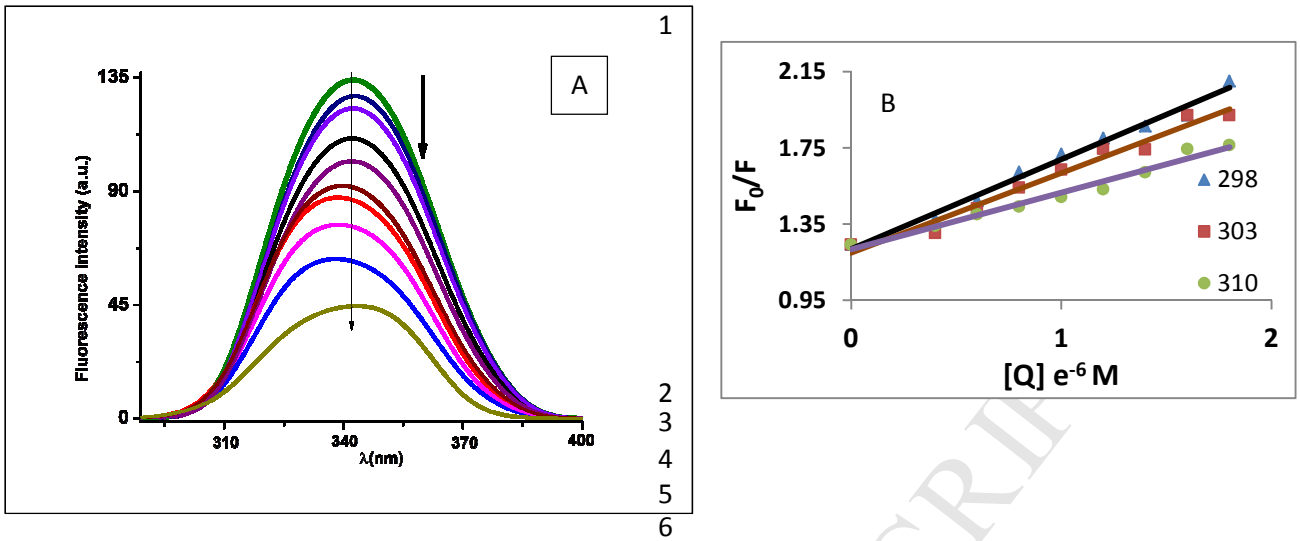

Fig.5. **a)** Fluorescence spectra of HSA (5µM) in the presence of HTp
Arrow shows concentration ranges from 0-45 µM at 298 K
b) SV curves for the binding of HTp-HSA at 298, 303 and 310 K at pH 7.4;
λ_{ex} = 280 nm; λ_{em} = 340 nm;

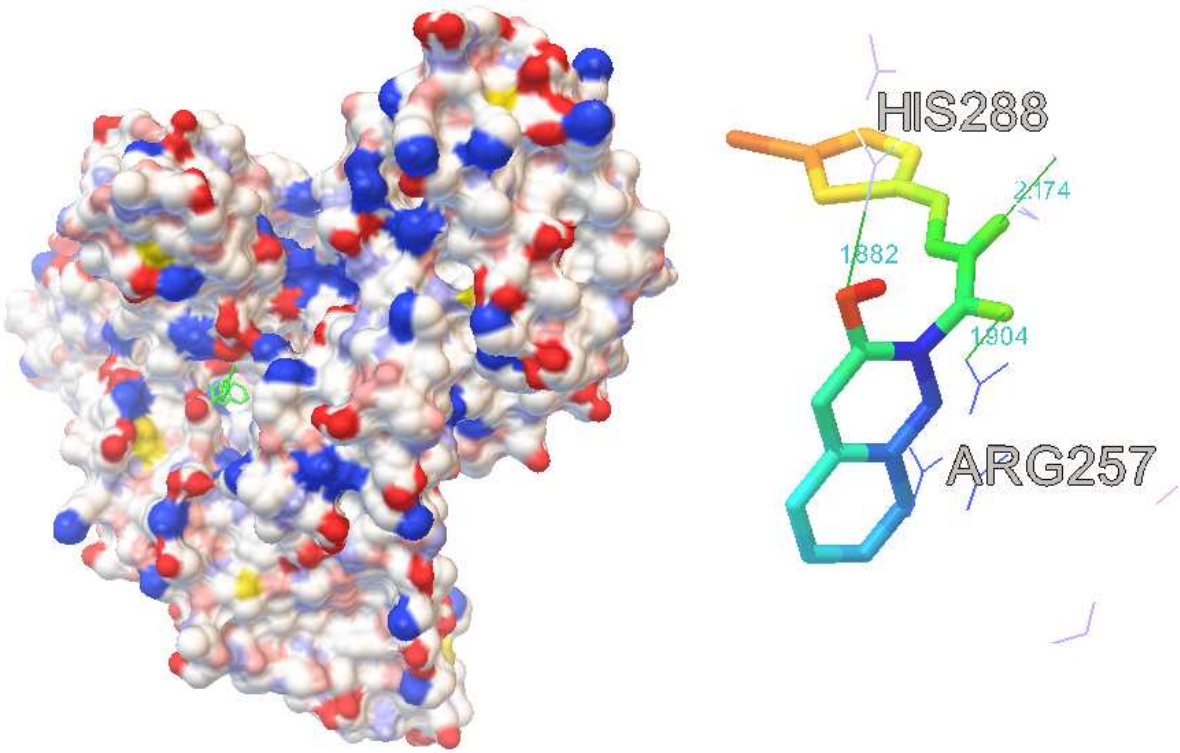

Fig.6. **(A)** Enfolding of molecule HTp in the active site pocket of Serum Albumin target (1H9Z)
(B) H-bond interaction of ligand molecule HTp with HSA.

Table.1: The quenching constants (K_{sv}), binding constants (K_b), number of binding sites (n) and corresponding correlation binding parameters for HSA-HTp interaction system at different temperatures obtained from fluorescence spectrophotometry

Compound	Temp (K)	$K_{sv} \times 10^4$ (L/mol)	$K_q \times 10^{12}$ (L/mol/sec)	$K_b \times 10^5$ (L/mol)	R^2	*SD	n
HTp	298	2.8355 ±0.24	2.8355±0.21	44.452±0.47	0.9942	0.012	1.0461
	303	2.7021±0.13	2.7021±0.44	37.132±0.35	0.9883	0.021	1.0320
	310	2.5801±0.57	2.5801±0.32	13.135±0.22	0.9801	0.024	1.1621

*R^2 =Correlation coefficient for the K_b, *SD -standard deviation of the best fit*

Table.2: Thermodynamic binding parameters for HSA-ligand interaction system at different temperatures.

Compound	Temp (K)	$K_b \times 10^5$ (L/mol)	ΔGº (KJ/mol)	ΔHº (KJ/mol)	ΔSº (J/K/mol)
HTp	298	44.452±0.47	-33.518	-78.314	-361.304
	303	37.132±0.35	-32.414		
	310	13.135±0.22	-29.186		

5. Bibliography

[1]. R.M. Mohareb, D.H. Fleita, O.K. Sakka, O. City, Novel Synthesis of Hydrazide-Hydrazone Derivatives and Their Utilization in the Synthesis of Coumarin, Pyridine, Thiazole and Thiophene Derivatives with Antitumor Activity, Acta Chim. Slov, 2013, (2011) 16–27. doi:10.3390/molecules16010016.

[2]. H.H. Monfared, O. Pouralimardan, C. Janiak, Synthesis and Spectral Characterization of Hydrazone Schiff Bases Derived from 2, 4-Dinitrophenylhydrazine. Crystal Structure of Salicylaldehyde-2,4-Dinitrophenylhydrazone, Z. Naturforsch, 62b (2007) 717–720.

[3]. Y. Lei, G. Chen, Q. Yang, C. Fu, J. Pan, T. Li, Synthesis And Structures Of Two Hydrazone Compounds Derived From 4-Methylbenzohydrazide, J. Struct. Chem., 54 (2013) 829–833. doi:10.1134/S0022476613040288.

[4]. A. Stadler, J. Harrowfield, Bis-acyl-/aroyl-hydrazones as multidentate ligands, Inorganica Chim. Acta, 362 (2009) 4298–4314. doi:10.1016/j.ica.2009.05.062.

[5]. S. Naseem, M. Khalid, M. Nawaz, M.A. Halim, A.A.C. Braga, M. Moazzam, Z. Sha, Synthesis, structural, DFT studies, docking and antibacterial activity of a xanthene-based hydrazone ligand, J. Mol. Struct. 1143 (2017) 235-244. doi:10.1016/j.molstruc.2017.04.093.

[6]. O.A. El-Gammal, Mononuclear and binuclear complexes derived from hydrazone Schiff base NON donor ligand : Synthesis, structure, theoretical and biological studies, Inorganica Chim. Acta. 435 (2015) 73–81. doi:10.1016/j.ica.2015.06.009.

[7]. G. Verma, A. Marella, M. Shaquiquzzaman, M. Akhtar, M. Rahmat Ali, M. Mumtaz Alam, J Pharm Bioallied Sci., 6 (2014) 69–80.

[8]. E. Colleen, A. Booth, A.C. Sartorelli, Inhibition of Deoxyribonucleotide Synthesis by Pyridine Carboxaldehyde Thiosemicarbazones, Cancer Res., 31 (1971) 235–239.

[9]. P. Kumar, D. Nandan, Spectral studies on cobalt(II), nickel(II) and copper(II) complexes of naphthaldehyde substituted aroylhydrazones, Spectrochim. Acta Part A, 64 (2006) 853–858. doi:10.1016/j.saa.2005.08.014.

[10]. H. Hosseini, R. Bikas, P. Mayer, Homogeneous green catalysts for olefin oxidation by mono oxovanadium(V) complexes of hydrazone Schiff base ligands, Inorganica Chim. Acta. 363 (2010) 2574–2583. doi:10.1016/j.ica.2010.04.046.

[11]. A. Ray, S. Banerjee, S. Sen, Ray J. Butcher, G.M. Rosair, M.T. Garland, S. Mitra, Two Zn(II) and one Mn(II) complexes using two different hydrazone ligands : spectroscopic studies and structural aspects, Struct. Chem., 19 (2008) 209–217. doi:10.1007/s11224-

007-9274-7.

[12]. R.M. Mohareb, N.S. Abbas, R.A. Ibrahim, New Approaches for the Synthesis of Thiophene Derivatives with Anti-tumor Activities, Acta Chim. Slov., (2013) 583–594.

[13]. L. Xu, Yan-Xi Hu, Yan-C. Li, Yu-F. Liu, Li Zhang, Hai-X. Ai, H. H. Liu, Study on the interaction of paeoniflorin with human serum albumin (HSA) by spectroscopic and molecular docking techniques, Chem. Cent. J., 11 (2017)116.

[14]. Z. Liu, X. Chen, Simple bioconjugate chemistry serves great clinical advances: albumin as a versatile platform for diagnosis and precision therapy, Chem. Soc. Rev., (2016) DOI: 10.1039/c5cs00158g

[15]. P. Zhao, G. Gao, L. Zhang, Q. Cai, N. Lu, L. Cheng, S. Li, X. Hou, Drug-protein binding mechanism of juglone for early pharmacokinetic profiling: Insights from ultrafiltration, multi-spectroscopic and molecular docking methods, J. Pharm. Biomed. Anal., 141 (2017) 262–269. doi:10.1016/j.jpba.2017.03.036.

[16]. a) H. Rimac, Z. Debelijak, D. Sakic, T. Weitner, M. Gabricevic, V. Vrcek, B. Zorc, M. Bojic, Structural and electronic determinants of flavonoid binding to human serum albumin: an extensive ligand-based study, RSC Adv., 6 (2016) 75014. DOI: 10.1039/c6ra17796d

b) S. Allosteric, I. Enantiomers, W. Warfarin, Stereoselective Binding Of 3-Acetoxy-, And 3-hydroxy-1,4-benzodiazepine-2-ones to Human Serum Albumin, Biochem. Pharmacol., 35 (1986) 263–269.

[17]. M. Dehkhodaei, M. Khorshidifard, H. Amiri, M. Sahihi, G. Azimi, N. Habibi, S. Taheri, G. Bruno, R. Azadbakht, Synthesis, characterization, crystal structure and DNA, HSA-binding studies of four Schiff base complexes derived from salicylaldehyde and isopropylamine, Inorg. Chim. Acta. 466 (2017) 48–60. doi:10.1016/j.ica.2017.05.035.

[18]. M.B. Bolattin, S.T. Nandibewoor, S.D. Joshi, S.R. Dixit, S.A. Chimatadar, Interaction of Hydralazine with Human Serum Albumin and Effect of β Cyclodextrin on Binding : Insights from Spectroscopic and Molecular Docking Techniques, Ind. Eng. Chem. Res., 55 (2016)5454-5464. doi:10.1021/acs.iecr.6b00517.

[19]. K. Savithri, B.C. Vasanth Kumar, H. D. Revanasiddappa, V. Hamse Kameshwar, M. Kaur, J.P. Jasinski, 2-((E)-(6-fluorobenzo[d]thiazol-2-ylimino) methyl)-4-chlorophenol; synthesis, characterization, crystal structure, Hirshfeld surface analysis and BSA binding studies, J. Mol. Struc., 1142 (2017) 293–303. doi:10.1016/j.molstruc.2017.04.050.

[20]. J.R. Lakowicz, G. Weber, Quenching of Fluorescence by Oxygen. A Probe for

Structural Fluctuations in Macromolecules, Biochem., 12 (1973) 4161–4170.

[21]. X. Fu, D. Liu, Y. Lin, W. Hu, Z. Mao, X. Le, Water-soluble DNA minor groove binders as potential chemotherapeutic agents: synthesis, characterization, DNA binding and cleavage, antioxidation, cytotoxicity and HSA interactions, Dalton Trans., 43 (2014) 8721–8737. doi:10.1039/c3dt53577k.

[22]. S.M. Al-barody, H. Ahmad, Synthesis, structural characterization and thermal studies of lanthanide complexes with Schiff base, Cogent Chem. 41 (2015) 1–11. doi:10.1080/23312009.2015.1093920.

[23]. Bruker, APEX2 and SAINT. Bruker AXS Inc, Madison, Wisconsin, USA (2009).

[24]. G.M. Sheldrick, A Short history of SHELX, Acta Cryst., A64, (2008) 112-122.

[25]. a) N. Keswani, S. Choudhary, N. Kishore, Quantitative aspects of recognition of the antibiotic drug oxytetracycline by bovine serum albumin; Calorimetric and spectroscopic studies, J. Chem. Thermodynamics, 58, (2013) 196-205

b) I. Matei, M. Hillebrand, Interaction of kaempferol with human serum albumin: A fluorescence and circular dichroism study, J. Pharm. Biomed. Anal. 51 (2010) 768–773.

[26]. G. M. Sheldrick, Crystal structure refinement with SHELX, Acta Cryst., C71, (2015) 3-8.

[27]. A. L. Spek, Structure validation in chemical crystallography, Acta Cryst., D65, (2009) 148-155.

[28]. S. K. Wolff, D. J. Grimwood, J. J. McKinnon, D. Jayatilaka, and M. A. Spackman, CrystalExplorer 3.0, University of Western Australia, Perth, Australia, (2001).

[29]. D.A. Links, Insight into supramolecular self-assembly directed by weak interactions in acetophenone derivatives : crystal structures and Hirshfeld surface analyses, Cryst. Eng. Comm. 13 (2011) 6728–6741. doi:10.1039/c1ce05670k.

[30]. Shamsuzzaman, H. Khanam, A. Mashrai, M. Asif, A. Ali, A. Barakat, Y. N. Mabkhot, synthesis, crystal structure, Hirshfeld surfaces and thermal, mechanical and dielectrical properties of cholest-5-ene, J. Taibah Uni. Sci., 11 (2017) 141-150. http://dx.doi.org/10.1016/j.jtusci.2016.01.001

[31]. K. Byadagi, M. Meti, S. Nandibewoor, S. Chimatadar, Investigation of binding behavior of procainamide hydrochloride with human serum albumin using synchronous, 3D fluorescence and circular dichroism, J. Pharm. Anal., 7 (2017) 103–109. doi:10.1016/j.jpha.2016.07.004.

[32]. L. Zhao, J. Liu, R. Guo, Q. Sun, H. Yang, H. Li, Investigating the interaction mechanism of fluorescent whitening agents to human serum albumin using saturation

transfer difference-NMR, RSC Adv. 7 (2017) 27796–27806. doi:10.1039/C7RA04008C

[33]. a) S. Yu, M. Schuchardt, M. Tolle, M. V. Der Giet, W. Zidek, J. Dzubiella, M. Ballauff, Interaction of human serum albumin with uremic toxins: a thermodynamic study, RSC Adv., 7 (2017) 27913. DOI: 10.1039/c7ra02838e

b) G. Yang, C. Li, A. Zeng, Y. Zhao, R. Yang, Fluorescence spectroscopy of osthole binding to human serum albumin, J. Pharm. Anal., 3 (2013) 200–204. doi:10.1016/j.jpha.2012.10.002.

[34]. B.C.Vasantha Kumar, Savithri K, Chandra, Manpreet Kaur, Jerry P. Jasinski, H.D. Revanasiddappa, 4-Chloro-2-(5,6-dihydro-benzo[4,5]imidazo[1,2-c]quinazolin-6-yl)-phenol (HL); synthesis, characterization, crystal structure, Hirshfeld surface analysis and BSA binding studies, J. Mol. Struc., 1173 (2018) 481-489.

[35]. a) G, Vignesh, R. Senthilkumar, P. Paul, V. S. Periasamy, M. A. Akbarshac, S. Arunachalam, Protein binding and biological evaluation of polymer-anchored cobalt(III) complex containing a 2,2'-bipyridine ligand, RSC Adv., 2014, 4, 57483

b) P. Zhao, G. Gao, L. Zhang, Q. Cai, N. Lu, L. Cheng, S. Li, X. Hou, Drug-protein binding mechanism of juglone for early pharmacokinetic profiling: Insights from ultrafiltration, multi-spectroscopic and molecular docking methods, J. Pharm. Biomed. Anal., 141 (2017) 262–269. doi:10.1016/j.jpba.2017.03.036.

[36]. G. Rabbani, M. H. Baig, E. J. Lee, Won-K. Cho, J. Y. Ma, I. Choi, Biophysical Study on the Interaction between Eperisone Hydrochloride and Human Serum Albumin Using Spectroscopic, Calorimetric, and Molecular Docking Analyses, Mol. pharmaceut., 14 (2017) 1656-1665. doi:10.1021/acs.molpharmaceut.6b01124.

[37]. I. Khosravi, F. Hosseini, M. Khorshidifard, M. Sahihi, Synthesis, characterization, crystal structure and HSA binding of two new N, O, O-donor Schiff-base ligands derived from dihydroxybenzaldehyde and tert -butylamine, J. Mol. Struct., 1119 (2016) 373–384. doi:10.1016/j.molstruc.2016.04.094.

[38]. C. Pontremoli, N. Barbero, S. Visentin, Insight into the interaction of Inhaled Corticosteroids (ICS) with human serum albumin: a spectroscopic-based study Carlotta, J. Pharm. Anal., (2017). doi:10.1016/j.jpha.2017.07.003.

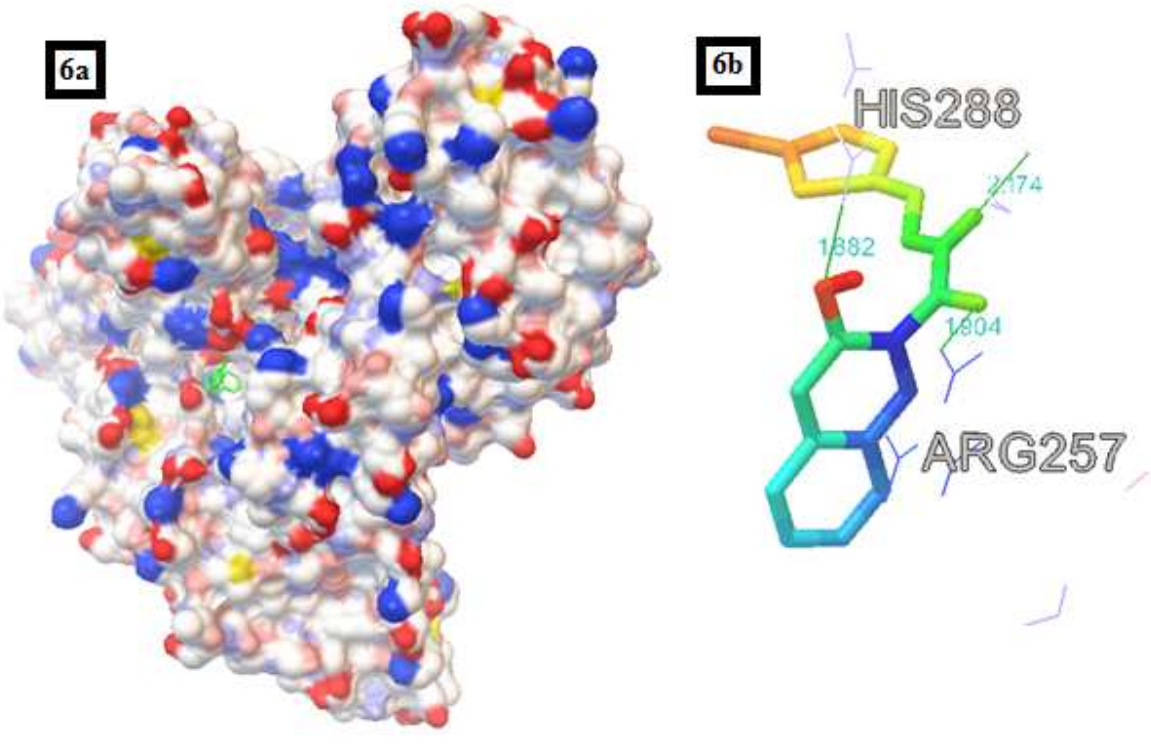

Fig.6. (A) Enfolding of molecule HTp in the active site pocket of Serum Albumin target (1H9Z)
(B) H-bond interaction of ligand molecule HTp with HSA.

Highlights:

1. The tridentate imine based molecule (HTp) was synthesized conveniently both by conventional and microwave methods.
2. Spectroscopic characterization, single x-ray crystallography and Hirshfeld surface mapping analysis for its structural elucidation.
3. Biological assays (HSA binding studies) for the potential analysis of prepared compound.
4. Results revealed that the synthesized molecule is an efficient protein binding drug exhibit higher binding affinity values was confirmed by both experimental (spectroscopic methods) and computational molecular docking simulation.